ENTANGLEMENT IN THE MIXED-THREE-SPIN XXX HEISENBERG MODEL WITH THE NEXT-NEAREST-NEIGHBOUR INTERACTION

Hamid Arian Zad

Department of Physics, Shahrood University of Technology
36155-316, Shahrood, Iran

(Received April 8, 2015; revised version received July 6, 2015; final version received July 17, 2015)

In this paper, we investigate thermal pairwise quantum correlation for any pair of spins of a mixed-three-spin XXX Heisenberg system (with spins connected together with the nearest-neighbour (NN) and that of the next-nearest-neighbour (NNN) coupling constants J_1 and J_2) by means of concurrence and quantum discord, as functions of temperature T, magnetic field B and the coupling constants J_2 and J_1. Some comparisons between these measures of entanglement are done for next-nearest-neighbour spins. We also express some magnetic properties and discuss the behaviour of the system in some special critical points. Some interesting and novel discussions are done to introduce some entanglement witnesses.

DOI:10.5506/APhysPolB.46.1911
PACS numbers: 03.65.Aa, 03.67.Mn, 75.10.Pq

1. Introduction

Quantum entanglement is one of the most interesting correlations [1, 2] which can exist only between quantum systems [3–5]. Recently, scientists are interested in entanglement for quantum systems such as the Heisenberg spin chains. This is because the Heisenberg spin chains are good candidates for studying the entanglement and simulating the nearest-neighbour interactions between quantum spins by verification some peculiar quantities [6]. For example, concurrence [7], negativity and quantum phase transition [8], quantum discord [9], quantum disorder (this subject has been precisely studied for the spin-1 Heisenberg chain in Ref. [10]), classical correlation, correlation functions, Von Neumann entropies [11], heat capacity and also in some cases with Dzyaloshinskii–Moriya (DM) interaction [12] for any pair of spins in the Heisenberg spin chains, have been studied [13–18]. The Heisenberg spin systems were used to study quantum dots [19, 20], entanglement controlling [21], and optical lattices [22]. In these references and in most of other papers, the NN interaction has been considered. Straightforward researches have been done about the next-nearest-neighbour interaction in the Heisenberg spin chains in Refs. [23, 24].

Recently, interesting investigations on the mixture of different spins have been reported in Refs. [17, 26]. In this work, we investigate pairwise entanglement for a mixed-three-spin (1/2,1,1/2) XXX Heisenberg chain with NN and NNN interaction in thermal equilibrium state, then introduce some special critical points which describe behaviours of this system in terms of the temperature T, the magnetic field B and the coupling constants changes. At first, we characterize the concurrence and the quantum discord in Sec. 2, in Sec. 3 we introduce our favourite model and represent circumstance of calculation of the Hamiltonian and density matrices. In Sec. 4, we will show numerical calculations and simulations of the pairwise entanglement for spins (1/2,1/2) (with NNN coupling constant J_2) and spins (1,1/2) (with NN coupling constant J_1) in terms of the temperature, the magnetic field and the coupling constants J_1 and J_2. After this, we usually use (sub)system $\mathcal{A}$ and (sub)system $\mathcal{B}$ term instead of the spins (1/2,1/2) and the spins (1,1/2) respectively. Section 5 concludes our main findings.

2. Measures of entanglement

Two powerful tools for verifying the pairwise entanglement of a bipartite system (in qubit–qubit or qubit–qutrit) are concurrence and quantum discord. We introduce them in this section.

2.1. Concurrence

The concurrence is a measure of entanglement, albeit only for states of two qubits [27] and it is defined as

$$C(\rho_{\mathcal{AB}}) = \max\left\{0, 2\lambda - \sum_{i=1}^{4} \lambda_i\right\}, \tag{1}$$

where $\lambda = \max\{\lambda_1, \lambda_2, \lambda_3, \lambda_4\}$ and λ_i are square roots of the eigenvalues of the inner product

$$R = \rho_{\mathcal{AB}}\tilde{\rho}_{\mathcal{AB}}, \tag{2}$$

with

$$\tilde{\rho}_{\mathcal{AB}} = (\sigma_y \otimes \sigma_y){\rho^\dagger}_{\mathcal{AB}}(\sigma_y \otimes \sigma_y) \tag{3}$$

for spins (1/2,1/2), and

$$\tilde{\rho}_{\mathcal{AB}} = (J_y \otimes \sigma_y){\rho^\dagger}_{\mathcal{AB}}(J_y \otimes \sigma_y) \tag{4}$$

for spins (1,1/2), where, on the standard basis, for a quantum system with Hamiltonian H in the thermal equilibrium state, ρ is defined as

$$\rho_{\mathrm{eq}} = \frac{\exp(-\beta H)}{\mathrm{Tr}[\exp(-\beta H)]}\,, \tag{5}$$

where β is $1/T$ (we here set $k_{\mathrm{B}} = 1$), T is the temperature and $Z = \mathrm{Tr}[\exp(-\beta H)]$ is the partition function of the system. $\rho^{\dagger}$ denotes the complex conjugation of density matrix ρ [29, 30] and

$$\sigma_y = \begin{pmatrix} 0 & -i \\ i & 0 \end{pmatrix}, \qquad J_y = \sqrt{2}\begin{pmatrix} 0 & -i & 0 \\ i & 0 & -i \\ 0 & i & 0 \end{pmatrix}. \tag{6}$$

According to the exact numerical calculations for Heisenberg spin models with NN spin interaction, plans of the concurrence and the quantum discord, with respect to the temperature and the magnetic field, have been presented in Ref. [16]. All these say us that if we have a system in a maximally entangled state, then $C(\rho_{\mathcal{AB}}) = 1$, while for a system in a separable state $C(\rho_{\mathcal{AB}}) = 0$. With regard to these plans, $C(\rho_{\mathcal{AB}})$ behaves as a sudden death at a critical temperature that is named "entanglement sudden death" (for more see Refs. [13, 32]). Moreover, in the finite temperatures and weak magnetic fields we also have a maximum amount of the concurrence, therefore the considered system has an entangled state in this region. We will investigate the concurrence and the quantum discord behaviours in some critical points for any pair of spins of the mixed-three-spin (1/2,1,1/2), with respect to the temperature, the magnetic field and the coupling constants J_1 and J_2. Then will present some interesting outcomes.

2.2. Quantum Discord (QD)

Let us review the Quantum Discord briefly. Total correlation in a bipartite quantum system with (sub)systems $\mathcal{A}$ and $\mathcal{B}$ is measured by quantum mutual information, which is defined as

$$I(\rho_{\mathcal{A}} : \rho_{\mathcal{B}}) = S(\rho_{\mathcal{A}}) + S(\rho_{\mathcal{B}}) - S(\rho_{\mathcal{AB}})\,. \tag{7}$$

The quantum mutual information has fundamental physical significance and is usually used as a measure of total correlations that include quantum information and classical ones (this subject has been precisely studied in Refs. [5, 32]). The classical correlation may be defined in terms of projective measurement. Suppose, we perform a set of projective measurements $\{\mathcal{B}^k\}$ on the (sub)system $\mathcal{B}$ with a set of complete projectors $\mathcal{B}^k$, then the probability of measurement outcome k may be defined as

$$p_k = \mathrm{Tr}_{\mathcal{AB}}\left[\left(I^{\mathcal{A}} \otimes \mathcal{B}^k\right)\rho_{\mathcal{AB}}\left(I^{\mathcal{A}} \otimes \mathcal{B}^k\right)\right], \tag{8}$$

where $I^{\mathcal{A}}$ is the identity operator for (sub)system $\mathcal{A}$. After this measurement, state of (sub)system $\mathcal{A}$ is described by the conditional density operator

$$\rho_k = \frac{1}{p_k}\left[\left(I^{\mathcal{A}} \otimes \mathcal{B}^k\right)\rho_{\mathcal{AB}}\left(I^{\mathcal{A}} \otimes \mathcal{B}^k\right)\right] . \tag{9}$$

The projectors $\mathcal{B}^k$ can be parametrized as $\mathcal{B}^k = \mathcal{V}|k\rangle\langle k|\mathcal{V}^\dagger$, where $k = 0, 1$ and the transform matrix $\mathcal{V}$ is

$$\mathcal{V} = \begin{pmatrix} \cos(\theta) & e^{-i\phi}\sin(\theta) \\ e^{i\phi}\sin(\theta) & -\cos(\theta) \end{pmatrix} , \tag{10}$$

where $0 \leq \theta \leq 2\pi$ and $0 \leq \phi \leq 2\pi$. We define the upper limit of the difference between the Von Neumann entropy $S(\rho_{\mathcal{A}})$ and the based-on-measurement quantum conditional entropy $S(\rho_{\mathcal{AB}}|\{\mathcal{B}^k\}) = \sum_k p_k S(\rho_k)$ of subsystem $\mathcal{A}$ *i.e.*,

$$\mathrm{CC}(\rho_{\mathcal{AB}}) = \sup_{\{\mathcal{B}^k\}}\left\{S\left(\rho_{\mathcal{A}}\right) - S\left(\rho_{\mathcal{AB}}|\left\{\mathcal{B}^k\right\}\right)\right\} , \tag{11}$$

then Quantum Discord is defined by $\mathrm{QD}(\rho_{\mathcal{AB}}) = I(\rho_{\mathcal{A}} : \rho_{\mathcal{B}}) - \mathrm{CC}(\rho_{\mathcal{AB}})$, therefore

$$\mathrm{QD}(\rho_{\mathcal{AB}}) = S(\rho_{\mathcal{A}}) - S(\rho_{\mathcal{AB}}) + S_{\min}(\rho_{\mathcal{AB}}) , \tag{12}$$

where $S_{\min}(\rho_{\mathcal{AB}}) = \min_{\{\mathcal{B}^k\}} S(\rho_{\mathcal{AB}}|\{\mathcal{B}^k\})$ [13]. The Quantum Discord and Classical Correlation have been verified in [14].

3. Mixed-three-spin (1/2,1,1/2) XXX Heisenberg model

We introduce Hamiltonian of the mixed-three-spin (1/2,1,1/2) system with NN and that of the NNN coupling constants, which in an external homogeneous magnetic field B is

$$H = J_1\left(\vec{S}_1 \cdot \vec{S}_2 + \vec{S}_2 \cdot \vec{S}_3\right) + J_2\left(\vec{S}_1 \cdot \vec{S}_3\right) + \sum_{i=1}^{3} \vec{B} \cdot \vec{S}_i , \tag{13}$$

where $\vec{S}_i = \{S_i^x, S_i^y, S_i^z\}$ for $i = 1, 3$ and $\vec{S}_2 = \{J_2^x, J_2^y, J_2^z\}$. J_1 and J_2 are the coupling constants between the spins (1,1/2) and the spins (1/2,1/2) respectively. $\vec{S}_i (i = 1, 2, 3)$ are spin operators (with $\hbar = 1$), which are introduced as the following equations:

$$S^x = \tfrac{1}{2}\begin{pmatrix} 0 & 1 \\ 1 & 0 \end{pmatrix} , \qquad S^y = \tfrac{1}{2}\begin{pmatrix} 0 & -i \\ i & 0 \end{pmatrix} , \qquad S^z = \tfrac{1}{2}\begin{pmatrix} 1 & 0 \\ 0 & -1 \end{pmatrix} , \tag{14}$$

$$J^x = \sqrt{2}\begin{pmatrix} 0 & 1 & 0 \\ 1 & 0 & 1 \\ 0 & 1 & 0 \end{pmatrix}, \qquad J^y = \sqrt{2}\begin{pmatrix} 0 & -i & 0 \\ i & 0 & -i \\ 0 & i & 0 \end{pmatrix},$$
$$J^z = \begin{pmatrix} 1 & 0 & 0 \\ 0 & 0 & 0 \\ 0 & 0 & -1 \end{pmatrix}. \tag{15}$$

Here, we consider $\vec{B} = B_z$ that is a homogeneous magnetic field in the z-direction. Note that the parameters introduced here are dimensionless. Eigenvectors of the Hamiltonian are

$$\begin{aligned}
|\,\phi_1\rangle &= |\,1/2,1,1/2\rangle\,, \\
|\,\phi_2\rangle &= |\,1/2,1,-1/2\rangle - \sqrt{2}\,|\,1/2,0,1/2\rangle + |\,-1/2,1,1/2\rangle\,, \\
|\,\phi_3\rangle &= |\,1/2,-1,-1/2\rangle - \sqrt{2}\,|\,-1/2,0,-1/2\rangle + |\,-1/2,-1,1/2\rangle\,, \\
|\,\phi_4\rangle &= |\,1/2,-1,-1/2\rangle + \sqrt{2}\,|\,-1/2,0,-1/2\rangle + |\,-1/2,-1,1/2\rangle\,, \\
|\,\phi_5\rangle &= |\,1/2,1,-1/2\rangle + \sqrt{2}\,|\,1/2,0,1/2\rangle + |\,-1/2,1,1/2\rangle\,, \\
|\,\phi_6\rangle &= |\,-1/2,-1,-1/2\rangle\,, \\
|\,\phi_7\rangle &= -\,|\,1/2,-1,1/2\rangle + |\,-1/2,1,-1/2\rangle\,, \\
|\,\phi_8\rangle &= |\,1/2,0,-1/2\rangle + \frac{\sqrt{2}}{2}(|\,1/2,-1,1/2\rangle + |\,-1/2,1,-1/2\rangle) \\
&\quad + |\,-1/2,0,1/2\rangle\,, \\
|\,\phi_9\rangle &= |\,1/2,0,-1/2\rangle - \sqrt{2}(|\,1/2,-1,1/2\rangle + |\,-1/2,1,-1/2\rangle) \\
&\quad + |\,-1/2,0,1/2\rangle\,, \\
|\,\phi_{10}\rangle &= -\,|\,1/2,-1,-1/2\rangle + |\,-1/2,-1,1/2\rangle\,, \\
|\,\phi_{11}\rangle &= -\,|\,1/2,1,-1/2\rangle + |\,-1/2,1,1/2\rangle\,, \\
|\,\phi_{12}\rangle &= -\,|\,1/2,0,-1/2\rangle + |\,-1/2,0,1/2\rangle\,,
\end{aligned} \tag{16}$$

and its eigenvalues are

$$\begin{aligned}
E_1 &= \tfrac{1}{4}J_2 + J_1 + 2B\,, & E_2 &= \tfrac{1}{4}J_2 - J_1 + B\,, & E_3 &= \tfrac{1}{4}J_2 - J_1 - B\,, \\
E_4 &= \tfrac{1}{4}J_2 + J_1 - B\,, & E_5 &= \tfrac{1}{4}J_2 + J_1 + B\,, & E_6 &= \tfrac{1}{4}J_2 + J_1 - 2B\,, \\
E_7 &= \tfrac{1}{4}J_2 - J_1\,, & E_8 &= \tfrac{1}{4}J_2 + J_1\,, & E_9 &= \tfrac{1}{4}J_2 - 2J_1\,, \\
E_{10} &= -\tfrac{3}{4}J_2 - B\,, & E_{11} &= -\tfrac{3}{4}J_2 + B\,, & E_{12} &= -\tfrac{3}{4}J_2\,.
\end{aligned} \tag{17}$$

In the standard states, we can characterize total density matrix of the considered system in the thermal equilibrium state, by using Eq. (13). Therefore, density matrix of any pair of spins can be expressed as

$$\rho_{23}^{T_1} = \frac{1}{Z}\begin{pmatrix} \alpha & 0 & 0 & 0 & 0 & 0 \\ 0 & A & \lambda & 0 & 0 & 0 \\ 0 & \lambda^* & D & 0 & 0 & 0 \\ 0 & 0 & 0 & F & \xi & 0 \\ 0 & 0 & 0 & \xi^* & G & 0 \\ 0 & 0 & 0 & 0 & 0 & \gamma \end{pmatrix}, \quad \rho_{13}^{T_2} = \frac{1}{Z}\begin{pmatrix} \delta & 0 & 0 & 0 \\ 0 & P & \zeta & 0 \\ 0 & \zeta^* & Q & 0 \\ 0 & 0 & 0 & \chi \end{pmatrix}, \tag{18}$$

where T_1 and T_2 are partial traces over first and second spins, respectively, (note that these matrices are symmetric). $\{\alpha, \lambda, \xi, \gamma, \delta, \zeta, \chi\}$ and $\{A, D, F, G, P, Q\}$ are functions of the T, B and J_2 with respect to the J_1, and also a mixture of total density matrix components that we analytically calculate using `Maple`$^{\mathrm{TM}}$ software.

4. Numerical calculations

Finally, we calculate numerically corresponding concurrences using Eq. (18) for (sub)systems $\mathcal{A}$ and $\mathcal{B}$, with respect to the temperature T and the coupling constant J_2 (Figs. 1 (a) and 2 (a)), and also with respect to the magnetic field B and the coupling constant J_2 (Figs. 1 (b) and 2 (b)), for finding critical temperatures and critical magnetic fields of which the concurrences vanish and the entanglement death occurs). Concurrences increase monotonously from zero to a maximum, with the decreasing of the temperature T and also with the increasing of the magnetic field B (note that our calculations are according to the changes of T, B and J_2 with respect to J_1).

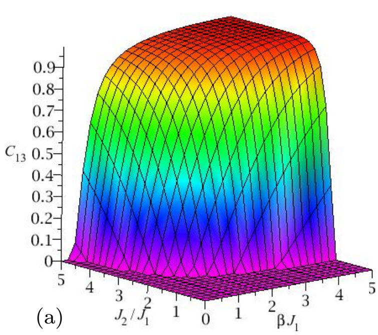

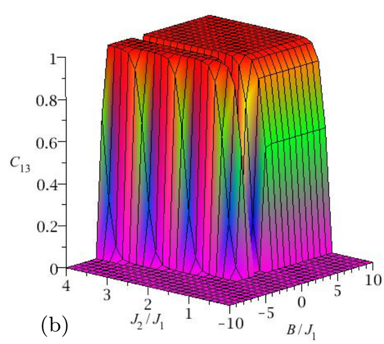

Fig. 1. Concurrence for (sub)system $\mathcal{A}$, (a) with respect to the temperature and J_2 at $B = J_1$, and (b) with respect to the magnetic field and J_2 at finite temperature ($T = 0.1J_1$). Note that here for $J_2 > J_1$ the concurrence does not vanishes at $B = 0$.

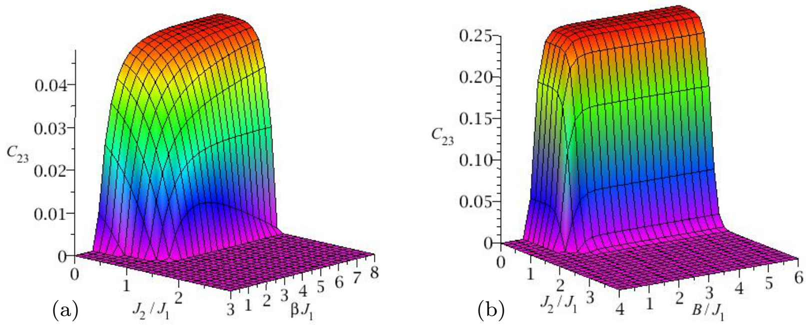

Fig. 2. Concurrence for (sub)system $\mathcal{B}$, (a) with respect to the temperature and J_2 at $B = J_1$, and (b) with respect to the magnetic field and J_2 at finite temperature ($T = 0.1J_1$).

In finite low temperatures ($T \ll J_1$) and strong magnetic fields ($B \gg J_1$), Figs. 1 (a) and (b) show that the concurrence between spins (1/2,1/2) increases and reaches the maximum, with the increasing of the coupling constant $J_2(J_2 > J_1)$, while Figs. 2 (a) and (b) show that the concurrence between spins (1,1/2) increases but with the decreasing of J_2 (from $J_2 \approx J_1$ to zero). So, for the favourite mixed-three-spin system, the concurrences are solely dependent on the coupling constant J_2.

It is mentioned that in the finite low temperatures and strong magnetic fields, the concurrences reach the maximum amounts, therefore ground states of (sub)systems $\mathcal{A}$ and $\mathcal{B}$ are entangled at $J_2 \gg J_1$ and $J_2 \ll J_1$ respectively. In the high temperatures and weak magnetic fields, they behave as an entanglement sudden death, just like concurrences which have been presented in Refs. [13, 16], but with an explicit difference that here, in the various magnetic fields, the entanglement sudden death occurs in the various critical temperatures, whereas in the previous works, it occurs in the identical critical temperature. This property of (sub)systems $\mathcal{A}$ and $\mathcal{B}$ is shown in Fig. 3. It is clear that, by the magnetic field changes, the entanglement sudden death occures at different critical temperatures, which means that the critical temperature is a function of the magnetic field.

Further, in Fig. 4 we plot critical temperature changes with respect to the coupling constant J_2, for both of (sub)systems $\mathcal{A}$ and $\mathcal{B}$. This figure shows that the critical temperature for (sub)system $\mathcal{A}$ increases with the increasing of the coupling constant J_2, but we see that this value decreases for (sub)system $\mathcal{B}$. The inset of Fig. 4 shows that the critical temperature reaches a permanent value for (sub)system $\mathcal{A}$ at the very high coupling constant $J_2(J_2 \gg J_1)$. Critical magnetic field changes with respect to the coupling constant J_2, for both of (sub)systems, which is shown in Fig. 5. This figure shows that critical magnetic field for (sub)system $\mathcal{A}$ decreases

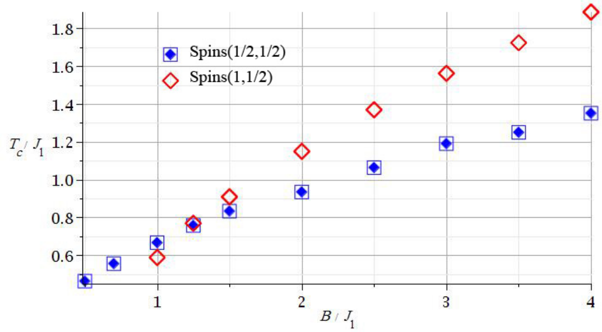

Fig. 3. The magnetic field dependence of the critical temperature T_{c} for (sub)systems $\mathcal{A}$ and $\mathcal{B}$.

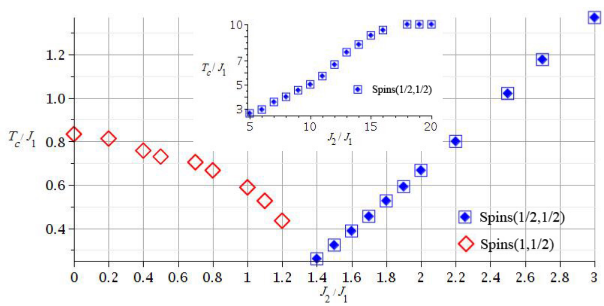

Fig. 4. The coupling constant J_2 dependence of the critical temperature T_{c} at $B = J_1$ for (sub)systems $\mathcal{A}$ and $\mathcal{B}$.

with the increasing of the coupling constant J_2, but this value increases for (sub)system $\mathcal{B}$. For $J_2 \gg J_1$, the critical magnetic field for (sub)system $\mathcal{A}$ reaches a permanent value, whereas at $J_2 \ll J_1$, the critical magnetic field is a permanent value for (sub)system $\mathcal{B}$.

Finally, we study the pairwise entanglement by verifying the quantum discord for (sub)system $\mathcal{A}$. This quantity is shown in Fig. 6. As illustrated in this figure, at finite temperatures and the high coupling constant J_2, we see that the quantum discord is in the maximum (just like its concurrence shown in Fig. 1). It means that the ground state of (sub)system $\mathcal{A}$ (in this area) is entangled, in other words, the spins (1/2,1/2) have a quantum correlation. This quantity decreases with the increasing of the temperature and decreasing of the J_2. Note that all of introduced figures both for the concurrence and the quantum discord are asymmetric.

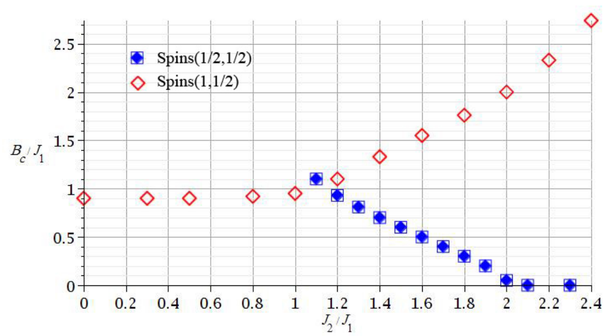

Fig. 5. The coupling constant J_2 dependence of the critical magnetic field B_{c} at the finite temperatures, for (sub)systems $\mathcal{A}$ and $\mathcal{B}$.

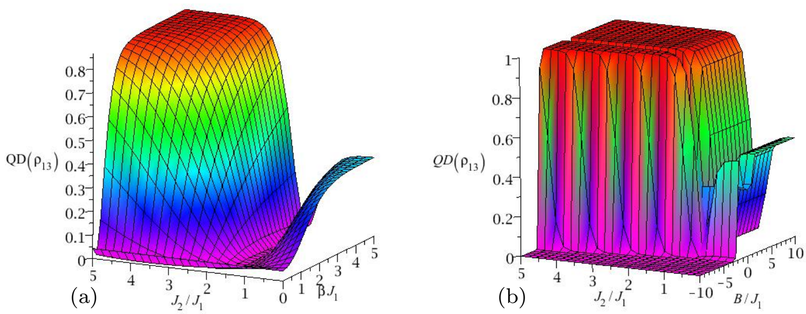

Fig. 6. Quantum discord for (sub)system $\mathcal{A}$, (a) with respect to the temperature and J_2 at $B = J_1$, and (b) with respect to the magnetic field and J_2 at finite temperature ($T = 0.1J_1$).

At infinite temperatures and the low coupling constant J_2 (Fig. 6 (a)) and also at weak magnetic fields and the low coupling constant J_2 (Fig. 6 (b)), the quantum discord does not vanish. This phenomenon represents power of this measure of entanglement for verifying quantum correlations between spins (1/2,1/2) rather than the concurrence.

Differences between the quantum discord and the concurrence for (sub)system $\mathcal{A}$ are shown in Figs. 7 and 8. As shown in these figures, we see that diagrams of the concurrence and the quantum discord are generally different. At the high coupling constant J_2, these diagrams are almost similar to each other at various temperatures (Fig. 7 (a)) and various magnetic fields (Fig. 7 (b)), but in the low coupling constant J_2, they have explicitly different behaviour, namely the concurrence at this range of J_2 vanishes completely, whereas the quantum discord does not vanishes completely.

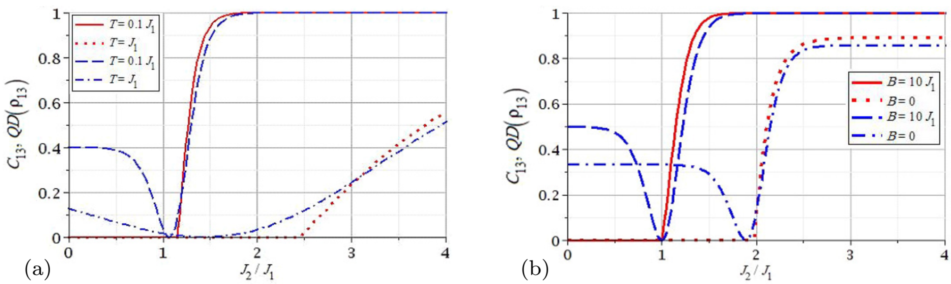

Fig. 7. The coupling constant J_2 dependence of the concurrence and the quantum discord for (sub)system $\mathcal{A}$, (a) at various temperatures and $B = J_1$, and (b) at various magnetic fields and finite temperature ($T = 0.1J_1$).

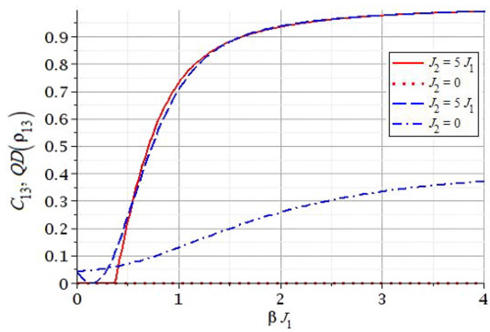

Fig. 8. Temperature dependence of the concurrence and the quantum discord for (sub)system $\mathcal{A}$ at the various coupling constant J_2 and $B = J_1$.

Comparison between the concurrence and the quantum discord *versus* temperature is presented in Fig. 8. As shown in this figure, at infinite temperatures, their diagrams are different from each other. One can see that the entanglement sudden death occurs in the concurrence diagrams, whereas it does not occur for the quantum discord diagrams (interestingly, the quantum discord does not vanish even at infinite temperatures and zero coupling constant J_2).

At the end of this paper, we present our new results about entanglement witnesses existence of our favourite system. Relationship between the temperature and the coupling constant J_2, also between the magnetic field and the coupling constant J_2, are shown in Figs. 9 and 10 for (sub)system $\mathcal{A}$ and (sub)system $\mathcal{B}$ respectively. These figures show a boundary between the entangled states and separable states (solid lines), therefore they can be considered as interesting entanglement witnesses.

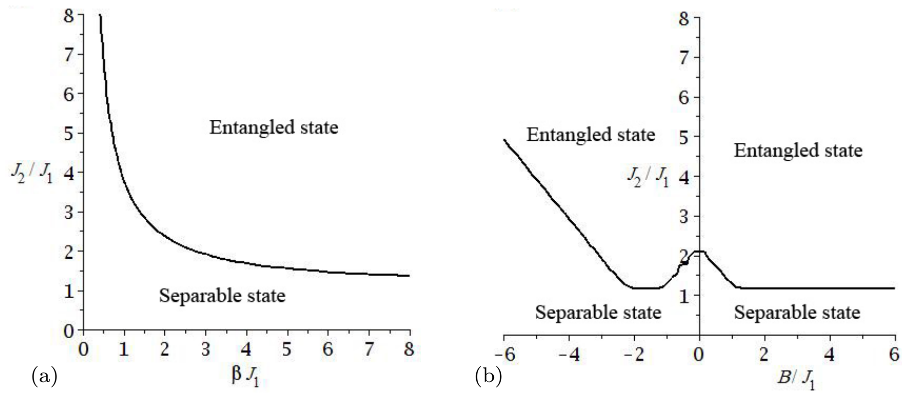

Fig. 9. Boundary between entangled states and separable states for (sub)system $\mathcal{A}$, (a) with respect to the temperature and the coupling constant J_2 at $B = J_2$, and (b) with respect to the magnetic field and the coupling constant J_2, at finite temperature ($T = 0.1J_1$).

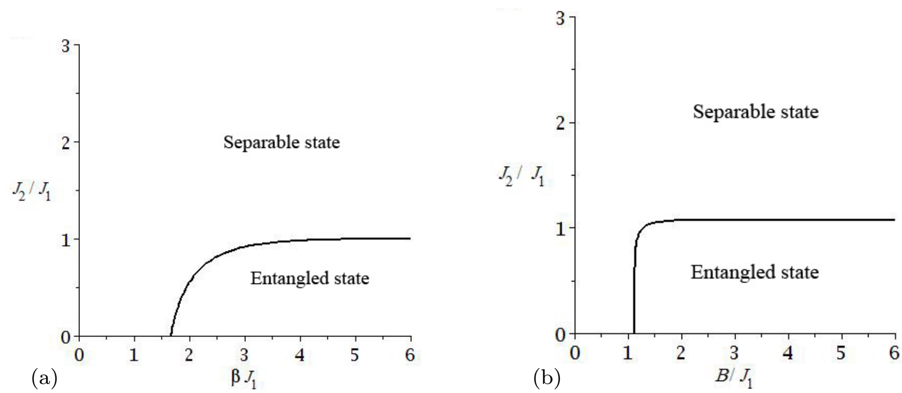

Fig. 10. Boundary between entangled states and separable states for (sub)system $\mathcal{B}$, (a) with respect to the temperature and the coupling constant J_2 at $B = J_2$, and (b) with respect to the magnetic field and the coupling constant J_2, at finite temperature ($T = 0.1J_1$).

5. Summary and discussion

In this work, we have investigated pairwise entanglement for a mixed-three-spin XXX Heisenberg model with the nearest-neighbour and the next-nearest-neighbour interactions, in an external homogeneous magnetic field B in thermal equilibrium state, by means of the concurrence for (sub)system $\mathcal{A}$ and (sub)system $\mathcal{B}$. In this way, the quantum discord has also been investigated for (sub)system $\mathcal{A}$.

Figures 1 (a) and 2 (a) show increment of the pairwise entanglement with the decreasing of the temperature T and increasing of the magnetic field B. With the increasing temperature pairwise entanglement vanishes gradually and in the high temperatures the (sub)systems become separable. We have verified the concurrences as functions of the coupling constants J_2 and the magnetic field B with respect to J_1 at the finite temperatures in Figs. 1 (b) and 2 (b). As shown in these figures, the concurrence for (sub)system $\mathcal{A}$ increases with the increasing of the $J_2 (J_2 > J_1)$, and reach the maximum at $J_2 \gg J_1$ and $B \gg J_1$, whereas the concurrence for (sub)system $\mathcal{B}$ increases with the decreasing of J_2 $(J_2 < J_1)$, and reach the maximum at $J_2 \ll J_1$ and $B \gg J_1$. One can see that the pairwise entanglement for (sub)system $\mathcal{A}$ is stronger than (sub)system $\mathcal{B}$, more generally, entanglement between the same spins is stronger than non-uniform spins.

We have also investigated the critical temperature T_{c} and the critical magnetic field B_{c} for both of the (sub)systems and obtained some interesting outcomes (see Figs. 3, 4 and 5). As illustrated in these figures, we see explicitly that the critical temperature is related to the magnetic field and the coupling constant J_2 (it increases with the increasing of the magnetic field). With the increasing of the coupling constant J_2, this parameter increases (decreases) (sub)system $\mathcal{A}$ ((sub)system $\mathcal{B}$). The critical magnetic field B_{c} (Fig. 4) changes with respect to the variations of the coupling constant J_2, for any of the (sub)systems.

Moreover, we have verified the quantum discord as a measure of entanglement for (sub)system $\mathcal{A}$, and have expressed some interesting and reasonable results by simulating it, as shown in Fig. 6. In this figure, one can find a good compatibility between our conclusions and previous interpretations of the quantum discord in Refs. [13, 14, 16], where at finite temperatures and $J_2 \gg J_1$, the quantum discord is in the maximum value for (sub)system $\mathcal{A}$.

Figure 6 (b) shows that the quantum discord decreases with the decreasing of the coupling constant J_2. Generally, with the increasing of the temperature and decreasing of the J_2, this measure of entanglement gradually decreases until it reaches the minimum value, but does not vanish at infinite temperatures (while the concurrence for both of the (sub)systems vanishes at special critical temperatures). Therefore, the quantum discord and the concurrence present different types of quantum correlations between spins (1/2,1/2).

The difference between the concurrence and the quantum discord was shown in Figs. 7 and 8. From these figures we can conclude that the quantum discord is strongly related to the ratio of the NNN and NN coupling constants (J_2 and J_1).

Finally, we have introduced relationship between the temperature and the coupling constant J_2, also between the magnetic field and the coupling constant J_2, as entanglement witnesses for both of the (sub)systems. We have also seen that these witnesses for (sub)systems $\mathcal{A}$ and $\mathcal{B}$ are generally different from each other. These conclusions are valid for XX, XXZ and XYZ models.

REFERENCES

[1] N.J. Cerf, C. Adami, *Fund. Theor. Phys.* **81**, 77 (1997).

[2] N.J. Cerf, C. Adami, *Phys. Rev. Lett.* **79**, 5194 (1997).

[3] M. Horodecki, J. Oppenheim, A. Winter, *Nature* **436**, 673 (2005) [`arXiv:quant-ph/0505062`].

[4] M. Horodecki, J. Oppenheim, A. Winter, *Commun. Math. Phys.* **269**, 107 (2007).

[5] N.J. Cerf, C. Adami, *Physica D* **120**, 62 (1998).

[6] R. Horodecki, P. Horodecki, M. Horodecki, K. Horodecki, *Rev. Mod. Phys.* **81**, 865 (2009).

[7] W.K. Wootters, *Quantum Inf. Comput.* **1**, 27 (2001).

[8] X. Wang, S.J. Gu, *J. Phys. A: Math. Theor.* **40**, 10759 (2007).

[9] H. Ollivier, W.H. Zurek, *Phys. Rev. Lett.* **88**, 017901 (2001).

[10] H.L.C. Grande, N. Laorencie, F. Alet, A.P. Vieira, *Phys. Rev. B* **89**, 134408 (2014).

[11] M.M. Wilde, *From Classical to Quantum Shannon Theory*, Cambridge University Press, 2013 [`arXiv:1106.1445 [quant-ph]`].

[12] Z. Xi, X.M. Lu, X. Wang, Y.J. Li, *J. Phys. A: Math. Theor.* **44**, 375301 (2011).

[13] T. Mamtimin *et al.*, *Chin. Phys. Lett.* **30**, 030303 (2013).

[14] K. Modi *et al.*, *Rev. Mod. Phys.* **84**, 1655 (2012).

[15] J.M. Moix, Y. Zhao, J. Cao, *Phys. Rev. B* **85**, 115412 (2012).

[16] W. Qiong, L.J. Qiao, Z.H. Sheng, *Chin. Phys. B* **19**, 100311 (2010).

[17] S.D. Han, E. Aydiner, *Chin. Phys. B* **23**, 050305 (2014).

[18] R. Dillenschneider, *Phys. Rev. B* **78**, 224413 (2008).

[19] H. Singh *et al.*, *New J. Phys.* **15**, 113001 (2013).

[20] G. Burkard, D. Loss, D.P. Vincenzo, *Phys. Rev. B* **59**, 2070 (1999).

[21] C.Z. Dong, *Chin. Phys. B* **17**, 1084 (2008).

[22] A. Abliz *et al.*, *Phys. Rev. A* **74**, 052105 (2006).

[23] W.M. Liu *et al.*, *Phys. Rev. Lett.* **88**, 170408 (2002).

[24] L.C. Kwek, Y. Takahas, K.W. Choo, *J. Phys.: Conf. Ser.* **143**, 012014 (2009).

[25] S.J. Gu, H. Li, Y.Q. Li, H.Q. Lin, *Phys. Rev. A* **70**, 052302 (2004).

[26] W.Q. Ning *et al.*, *J. Phys. Condens. Matter* **20**, 235236 (2008).

[27] D. McMahon, *Quantum Computing Explained*, John Wiley & Sons, New York 2008.

[28] A.K. Pathria, *Statistical Mechanics*, Licensing Agency Ltd, 2^{th} Edition, London 1997.

[29] G.B. Furman, V.M. Meerovich, V.L. Sokolovsky, *Quantum. Inf. Process* **11**, 1603 (2012).

[30] G.B. Furman, V.M. Meerovich, V.L. Sokolovsky, *Quantum. Inf. Process* **10**, 307 (2011).

[31] C.J. Shan *et al.*, *Chin. Phys. Lett.* **25**, 3115 (2008).

[32] S.M. Barnett, *Quantum Information*, Oxford University Press, New York 2009.